DRAFT VERSION MAY 23, 2018
Typeset using LaTeX **twocolumn** style in AASTeX62

Evidence of Intermediate-Scale Energy Spectrum Anisotropy of Cosmic Rays $E \geq 10^{19.2}$ eV with the Telescope Array Surface Detector

R.U. ABBASI,[1] M. ABE,[2] T. ABU-ZAYYAD,[1] M. ALLEN,[1] R. AZUMA,[3] E. BARCIKOWSKI,[1] J.W. BELZ,[1] D.R. BERGMAN,[1] S.A. BLAKE,[1] R. CADY,[1] B.G. CHEON,[4] J. CHIBA,[5] M. CHIKAWA,[6] A. DI MATTEO,[7] T. FUJII,[8] K. FUJITA,[9] M. FUKUSHIMA,[8,10] G. FURLICH,[1] T. GOTO,[9] W. HANLON,[1] M. HAYASHI,[11] Y. HAYASHI,[9] N. HAYASHIDA,[12] K. HIBINO,[12] K. HONDA,[13] D. IKEDA,[8] N. INOUE,[2] T. ISHII,[13] R. ISHIMORI,[3] H. ITO,[14] D. IVANOV,[1] H.M. JEONG,[15] S. JEONG,[15] C.C.H. JUI,[1] K. KADOTA,[16] F. KAKIMOTO,[3] O. KALASHEV,[17] K. KASAHARA,[18] H. KAWAI,[19] S. KAWAKAMI,[9] S. KAWANA,[2] K. KAWATA,[8] E. KIDO,[8] H.B. KIM,[4] J.H. KIM,[1] J.H. KIM,[20] S. KISHIGAMI,[9] S. KITAMURA,[3] Y. KITAMURA,[3] V. KUZMIN,[17,*] M. KUZNETSOV,[17] Y.J. KWON,[21] K.H. LEE,[15] B. LUBSANDORZHIEV,[17] J.P. LUNDQUIST,[1] K. MACHIDA,[13] K. MARTENS,[10] T. MATSUYAMA,[9] J.N. MATTHEWS,[1] R. MAYTA,[9] M. MINAMINO,[9] K. MUKAI,[13] I. MYERS,[1] K. NAGASAWA,[2] S. NAGATAKI,[14] R. NAKAMURA,[22] T. NAKAMURA,[23] T. NONAKA,[8] A. NOZATO,[6] H. ODA,[9] S. OGIO,[9] J. OGURA,[3] M. OHNISHI,[8] H. OHOKA,[8] T. OKUDA,[24] Y. OMURA,[9] M. ONO,[14] R. ONOGI,[9] A. OSHIMA,[9] S. OZAWA,[18] I.H. PARK,[15] M.S. PSHIRKOV,[17,25] D.C. RODRIGUEZ,[1] G. RUBTSOV,[17] D. RYU,[20] H. SAGAWA,[8] R. SAHARA,[9] K. SAITO,[8] Y. SAITO,[22] N. SAKAKI,[8] N. SAKURAI,[9] L.M. SCOTT,[26] T. SEKI,[22] K. SEKINO,[8] P.D. SHAH,[1] F. SHIBATA,[13] T. SHIBATA,[8] H. SHIMODAIRA,[8] B.K. SHIN,[9] H.S. SHIN,[8] J.D. SMITH,[1] P. SOKOLSKY,[1] B.T. STOKES,[1] S.R. STRATTON,[1,26] T.A. STROMAN,[1] T. SUZAWA,[2] Y. TAKAGI,[9] Y. TAKAHASHI,[9] M. TAKAMURA,[5] R. TAKEISHI,[15] A. TAKETA,[27] M. TAKITA,[8] Y. TAMEDA,[28] H. TANAKA,[9] K. TANAKA,[29] M. TANAKA,[30] S.B. THOMAS,[1] G.B. THOMSON,[1] P. TINYAKOV,[17,7] I. TKACHEV,[17] H. TOKUNO,[3] T. TOMIDA,[22] S. TROITSKY,[17] Y. TSUNESADA,[3] K. TSUTSUMI,[3] Y. UCHIHORI,[31] S. UDO,[12] F. URBAN,[32] T. WONG,[1] M. YAMAMOTO,[22] R. YAMANE,[9] H. YAMAOKA,[30] K. YAMAZAKI,[12] J. YANG,[33] K. YASHIRO,[5] Y. YONEDA,[9] S. YOSHIDA,[19] H. YOSHII,[34] Y. ZHEZHER,[17] AND Z. ZUNDEL[1]

[1] *High Energy Astrophysics Institute and Department of Physics and Astronomy, University of Utah, Salt Lake City, Utah, USA*
[2] *The Graduate School of Science and Engineering, Saitama University, Saitama, Saitama, Japan*
[3] *Graduate School of Science and Engineering, Tokyo Institute of Technology, Meguro, Tokyo, Japan*
[4] *Department of Physics and The Research Institute of Natural Science, Hanyang University, Seongdong-gu, Seoul, Korea*
[5] *Department of Physics, Tokyo University of Science, Noda, Chiba, Japan*
[6] *Department of Physics, Kindai University, Higashi Osaka, Osaka, Japan*
[7] *Service de Physique Thorique, Universit Libre de Bruxelles, Brussels, Belgium*
[8] *Institute for Cosmic Ray Research, University of Tokyo, Kashiwa, Chiba, Japan*
[9] *Graduate School of Science, Osaka City University, Osaka, Osaka, Japan*
[10] *Kavli Institute for the Physics and Mathematics of the Universe (WPI), Todai Institutes for Advanced Study, University of Tokyo, Kashiwa, Chiba, Japan*
[11] *Information Engineering Graduate School of Science and Technology, Shinshu University, Nagano, Nagano, Japan*
[12] *Faculty of Engineering, Kanagawa University, Yokohama, Kanagawa, Japan*
[13] *Interdisciplinary Graduate School of Medicine and Engineering, University of Yamanashi, Kofu, Yamanashi, Japan*
[14] *Astrophysical Big Bang Laboratory, RIKEN, Wako, Saitama, Japan*
[15] *Department of Physics, Sungkyunkwan University, Jang-an-gu, Suwon, Korea*
[16] *Department of Physics, Tokyo City University, Setagaya-ku, Tokyo, Japan*
[17] *Institute for Nuclear Research of the Russian Academy of Sciences, Moscow, Russia*
[18] *Advanced Research Institute for Science and Engineering, Waseda University, Shinjuku-ku, Tokyo, Japan*
[19] *Department of Physics, Chiba University, Chiba, Chiba, Japan*
[20] *Department of Physics, School of Natural Sciences, Ulsan National Institute of Science and Technology, UNIST-gil, Ulsan, Korea*
[21] *Department of Physics, Yonsei University, Seodaemun-gu, Seoul, Korea*
[22] *Academic Assembly School of Science and Technology Institute of Engineering, Shinshu University, Nagano, Nagano, Japan*
[23] *Faculty of Science, Kochi University, Kochi, Kochi, Japan*
[24] *Department of Physical Sciences, Ritsumeikan University, Kusatsu, Shiga, Japan*
[25] *Sternberg Astronomical Institute, Moscow M.V. Lomonosov State University, Moscow, Russia*
[26] *Department of Physics and Astronomy, Rutgers University - The State University of New Jersey, Piscataway, New Jersey, USA*
[27] *Earthquake Research Institute, University of Tokyo, Bunkyo-ku, Tokyo, Japan*
[28] *Department of Engineering Science, Faculty of Engineering Osaka Electro-Communication University, Osaka, Osaka, Japan*
[29] *Graduate School of Information Sciences, Hiroshima City University, Hiroshima, Hiroshima, Japan*
[30] *Institute of Particle and Nuclear Studies, KEK, Tsukuba, Ibaraki, Japan*

Corresponding author: J.P. Lundquist
jplundquist@cosmic.utah.edu

[31] National Institute of Radiological Science, Chiba, Chiba, Japan
[32] Central European Institute for Cosmology and Fundamental Physics, Institute of Physics, Czech Academy of Sciences, Na Slovance 1999/2 Prague, Czech Republic
[33] Department of Physics and Institute for the Early Universe, Ewha Womans University, Seodaaemun-gu, Seoul, Korea
[34] Department of Physics, Ehime University, Matsuyama, Ehime, Japan

Submitted to ApJ

ABSTRACT

Evidence for an intermediate-scale energy spectrum anisotropy has been found in the arrival directions of ultra-high energy cosmic rays for energies greater than $10^{19.2}$ eV in the northern hemisphere using 7 years of Telescope Array surface detector data. A relative energy distribution test is done comparing events inside oversampled spherical caps of equal exposure, to those outside, using the Poisson likelihood ratio. The center of maximum significance is at 9^h16^m, 45°, and has a deficit of events with energies $10^{19.2}\leq E<10^{19.75}$ eV and an excess for $E\geq10^{19.75}$ eV. The post-trial probability of this energy anisotropy, appearing by chance anywhere on an isotropic sky, is found by Monte Carlo simulation to be 9×10^{-5} ($3.74\sigma_{global}$).

Keywords: astroparticle physics, cosmic rays, large-scale structure of universe

1. INTRODUCTION

Though the origin of ultra-high energy cosmic rays (UHECR) are still unknown, galactic sources are improbable because of the lack of strong anisotropy at energies above 10^{19} eV. Due to cosmic ray particle interactions with the infrared and microwave background radiation UHECR source distributions should be limited to distances less than 100 Mpc for protons and iron and intermediate mass nuclei like helium/oxygen/carbon/nitrogen limited to 20 Mpc (Kotera & Olinto (2011)). The number of possible accelerators in this volume is limited by energy considerations to galaxy clusters, active galaxy jets and lobes, supermassive black holes (AGNs), gamma-ray bursts, magnetars, and starburst galaxies.

These extragalactic objects are mainly distributed along the local large scale structure (LSS), most evidently along the "supergalactic plane." Nearby AGNs are concentrated around LSS with typical clustering lengths of 5–15 Mpc and a density a few hundred percent of the average within a 20° radius (Ajello et al. (2012)). This suggests that an intermediate-scale event density anisotropy may have a similar angular scale.

In fact a "Hotspot" 20° in size near Ursa Major has been observed by the Telescope Array (TA) experiment with a 3.4σ significance (Abbasi et al. (2014a)). The maximum of this event overdensity is at 9^h48^m, 43° for event energies greater than 57 EeV.

The present paper is an extension to lower energies ($E<57$ EeV) and is specifically a search for localized differences in the energy distribution of events within the field of view (FOV) with no assumptions from previous results. [1] The energy spectrum anisotropy found could be a signature of sources and intervening electromagnetic fields, and could, in principle, assume any shape.

2. EXPERIMENT

The TA experiment in Millard County, Utah (39.3° N, 112.9° W) consists of three fluorescence detectors (FD) and a surface detector (SD) array (Abu-Zayyad et al. (2013a); Tokuno et al. (2012)). The SD array has 507 plastic scintillation detectors, each 3 m^2 in area, placed on a 1.2 km spaced square grid resulting in a 700 km^2 collection area that makes it the northern hemispheres largest cosmic-ray detector. Data has been collected since 2008 with close to a 100% duty cycle. Less than 10% of SD data is observed in coincidence with the FD and it is used to calibrate the SD energy scale using the calorimetric fluorescence technique.

3. DATA SET

For this analysis SD data taken between May 11 of 2008 and 2015 is used. The reconstruction of these events is done in the same manner as the "Hotspot" analysis of Abbasi et al. (2014a). However, tighter data cuts are required to improve the zenith angle resolution because of the inclusion of lower energy events. The energy of reconstructed events is determined by SD and renormalized by 1/1.27 to match the FD energy scale that is determined calorimetrically (Abu-Zayyad et al. (2013b)).

Events are kept if they match the following criteria:

1. $E\geq10^{19.0}$ eV (where detection efficiency is ∼100%).

* Deceased

[1] The results of this analysis were first presented at the 35th International Cosmic Ray Conference ICRC2017 (Lundquist (2017)).

2. At least four SDs triggered.

3. Zenith angle of arrival direction <55°.

4. Reconstructed pointing direction error <5°.

5. Core distance >1.2 km from array boundary.

6. Shower lateral distribution fit χ^2/dof<10.

After cuts, there are 3027 data events in the set.

There is good agreement between the resulting data and theoretical distributions for the zenith angle (g(θ) = sin(θ)cos(θ)), azimuthal angle (uniform), and the energy spectrum which agrees with the published spectrum (Abu-Zayyad et al. (2013b); Abbasi et al. (2015)).

After cuts, energy resolution and zenith angle resolution of events range from 10 to 20% and 1.0° to 1.5° respectively, depending on core distance from array boundary and energy. These are reasonable resolutions for an intermediate-scale anisotropy search.

4. ISOTROPIC SIMULATION

Each Monte Carlo (MC) and data event is defined by their energy, zenith angle, azimuthal angle, and time. The latitude and longitude are defined from the center of TA at 39.3° Long., 112.9° Lat. Right Ascension (R.A.) and Declination (Dec.) equatorial coordinates are found using these variables (Vallado (2007)).

Each MC set energy distribution is sampled by interpolation from a set of 386,125 MC events, with energies E≥$10^{19.0}$ eV, reconstructed through an SD simulation that takes into account detector acceptance, on-time, and bias in the energy spectrum. This large MC set was created with the average HiRes spectrum (Abbasi et al. (2008)) and was also used for the TA spectrum measurement (Ivanov (2012)).

The MC event sets have a zenith angle distribution of g(θ) = sin(θ)cos(θ) due to the event sampling response of a flat SD array and a uniform azimuth distribution. On-time is simulated by randomly sampled trigger times from 246,499 data events with E>$10^{17.7}$ eV.

The result is that each set of MC events simulate the expectation for data from an isotropoic distribution based on the detector response and on-time. These MC sets are then used to calculate the final global significance of any potential anisotropy in the data.

5. METHOD

5.1. *Oversampling Anisotropy*

The oversampling method used in this paper is a modification of the large-scale anisotropy analysis developed by AGASA (Hayashida et al. (1999a); Hayashida et al. (1999b)), that is, an analysis done within overlapping spherical cap bins on the sky. The TA and HiRes collaborations have used similar methods previously (Abbasi et al. (2014a); Kawata et al. (2013); Ivanov & Thomson (2008)).

5.1.1. *Grid*

The oversampling is done on an equal opening angle grid with a median spacing of 0.5°±0.04°. This spacing ensures uniform coverage of the FOV and minimizes declination dependent sampling bias. While the FOV extends to -16°, the grid is terminated at 10° to avoid problems with the size of the spherical bins described in the next section.

5.1.2. *Equal Exposure Spherical Caps*

There is a sample size bias in distribution tests of flux, such as χ^2's and likelihood ratios, that creates a declination bias in the calculated significances if the sample size of the expectation changes with declination. The zenith angle exposure (g(θ) = sin(θ)cos(θ)) creates precisely this kind of bias if the spherical cap bin sizes are constant. In this case the isotropic expected number of events increases with declination. An equal exposure binning is adopted such that the exposure ratio $\alpha = N_{on}/N_{off}$ (Gillessen & Harney (2005)) is a constant value at each grid point.

A 2×10^7 MC event set is used to determine the three parameter fit of the cap bin sizes, the average bin size (15.0°, 20.0°, 25.0°, and 30.0°), and the constant α exposure ratio that results in the required average bin size. After the bin sizes are found each exposure ratio α map is calculated from a 5×10^7 MC event set to account for any remaining small variations from the bin size fit.

Smaller bin sizes do not have enough statistics inside them, and larger bin sizes start to lose sufficient statistics outside, for a meaningful distribution comparison. It is also the case that a 35° bin size covers more than 50% of the oversampling grid and is no longer "intermediate-scale." Furthermore, larger bin sizes have a greater change in shape at low declinations due to the exposure FOV cutoff.

Figure 1 shows the constant exposure ratio binning, α = 14.03%, that maximizes the data pre-trial significance which is an average bin size of 30.0°. Ratios of 3.35%, 6.04%, 9.58%, and 14.03% were tested to maximize the data pre-trial significance (the 15.0° to 30.0° spherical cap bin averages). This is a free parameter that the post-trial significance calculation takes into account.

5.2. *Energy Distribution Comparison Test*

The significance of a localized energy spectrum deviation is calculated using the binned Poisson likelihood ratio goodness of fit (GOF) test to compare the energy distribution inside each spherical cap to that outside the cap (Baker & Cousins (1984); Olive et al. (2014)). This is a GOF test that allows a low number of events in each energy bin, for both the observed (N_{on} inside the bin), and expected (N_{bg} normalized events outside) energy distributions.

Equation 1a shows this test in terms of observed energy bin frequencies, n_i, expected frequencies, μ_i, and exposure ratio α. The likelihood ratio is approximated by $-\chi^2/2$ with degrees of freedom (DOF) $dof = \#bins+2$ and is used to calculate the local pre-trial σ significance. There are two additional DOF due to the estimated background and the combining of low statistic energy bins described below. This was confirmed by MC simulation to follow the correct χ^2 distribution.

$$\chi^2 \simeq 2\sum_i \mu_i - n_i + n_i ln(n_i/\mu_i) \quad (1a)$$

$$N_{on} = \sum_i n_i \quad (1b)$$

$$N_{bg} = \sum_i \mu_i = \alpha(N_{events} - N_{on}) \quad (1c)$$

The choice of an energy bin width of 0.05 $\log_{10}$(E/eV) is *a priori* based on the detector energy resolution as it is slightly smaller than the average resolution for energies 10^{19}≤E≤$10^{20.4}$ eV.

The bias against the exact single bin χ^2 distribution is less than +15% for μ_i>2, and drops to +5% at expectations of 5 events in a bin (Heinrich (2001)). If the expected number of events in an energy bin is less than 1 (μ_i<1) it is combined with alternating adjacent bins. The resulting smallest energy bin expectations are greater than 2 (μ_i>2). The combining of bins with μ_i<1 ensures that the bias is positive for all bins instead of negative for the high energy bins with small expectations. This bias is smaller than other possible tests, is present for all locations on the sky map, and also present in the MC trials when calculating the global post-trial significance.

The expected energy spectrum is estimated by the histogram of events outside the spherical cap (N_{off}) that is normalized to the expected background number of events inside the cap (N_{bg}) using the method of Li & Ma (1983).

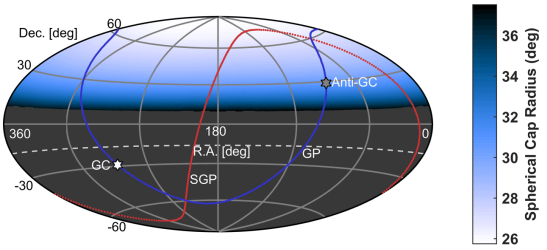

Figure 1. Equatorial Hammer-Aitoff projection of spherical cap bin sizes with an exposure ratio of $\alpha = 14.03\%$. The average bin radius is 30.0°. The dashed curve at Dec. = -16° defines the FOV.

The exposure ration ($\alpha = N_{on}/N_{off}$) at each point of the grid is calculated using a set of 5×10^7 isotropic MC events. The background is then estimated using the data as $N_{bg} = \alpha N_{off} = \alpha(N_{events} - N_{on})$. This depends on the data N_{on} inside each cap bin (Gillessen & Harney (2005)).

The lowest energy threshold tested to maximize the pre-trial significance was $10^{19.0}$ eV as the detection efficiency is ∼100% above this energy. Above $10^{19.4}$ eV there are only 546 events which is insufficient statistics for this analysis. The maximum significance is found to be for energies E≥$10^{19.2}$ eV. This is a free parameter and the appropriate penalty factor for this scan is taken as described in Section 6.3.

There are 1332 events above $10^{19.2}$ eV in the data set; 1248 with energy $10^{19.2}$≤E<$10^{19.75}$ eV and 84 with E≥$10^{19.75}$ eV. An energy threshold of $10^{19.75}$ eV (more exactly 57 EeV) was used for the TA Hotspot analysis as determined by the AGN correlation results from the Pierre Auger Observatory (PAO) (Abu-Zayyad et al. (2013c)).

6. RESULTS

6.1. *Density Map*

Figure 2(a) shows a projection of the 1332 cosmic-ray events observed by the SD with energies E≥$10^{19.2}$ eV. The oversampled number of events, N_{on}, using the 14.03% equal exposure caps is shown in Figure 2(b). This corresponds to an average cap size of 30° as discussed in Section 5.1.

6.2. *Local Energy Anisotropy Significance*

The pre-trial significance of local relative energy distribution deviations is calculated using the method of Section 5.2. Inside each spherical cap bin the energy distribution of events (N_{on}) is compared to that outside (N_{off}) by the Poisson likelihood GOF test (Equation 1a). The μ_i are the N_{off} energy histogram frequencies normalized to the expected number of events (N_{bg}) by Equation 1c. The α parameter is the exposure ratio described in Section 5.1.2.

Figure 3 shows the resulting local pre-trial energy anisotropy significance. This is with an energy threshold of E≥$10^{19.2}$ eV and the 14.03% equal exposure caps. The maximum pre-trial significance is 7° from the published Hotspot location (Abbasi et al. (2014a)) and corresponds to a $6.17\sigma_{local}$ at 9^h16^m, 45°.

The histogram of events inside the cap bin at maximum significance compared to the expected energies is shown in Figure 4 with, and without, the rebinning discussed in Section 5.2. Individual bin contributions to the statistical significance show an excess of events E≥$10^{19.75}$ eV (27 observed, 8 expected, $\chi^2/dof = 38.1/5$), and a "Coldspot" deficit of events $10^{19.2}$≤E<$10^{19.75}$ eV (120 observed, 158 expected, $\chi^2/dof = 40.2/12$). This shows that the contribution to the overall significance from these two energy ranges are roughly

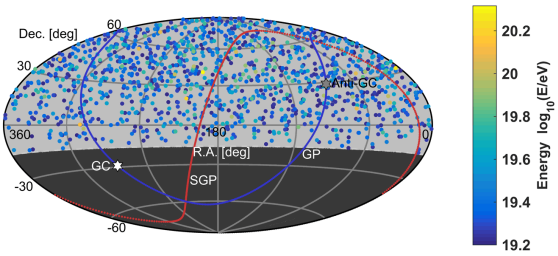

(a)

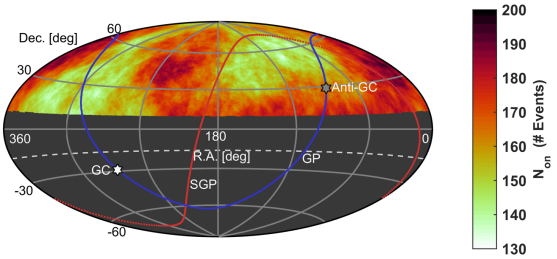

(b)

Figure 2. Projections of UHECR events in the data set. (a) Scatter plot of events colored by $\log_{10}$(E/eV). (b) Number of observed events, N_{on}, at each grid point, inside 14.03% equal exposure bins of the radius shown in Figure 1. There is an event deficit at the previously reported Hotspot location (9^h48^m, 43°). The dashed curve at Dec. = -16° defines the FOV. Solid curves indicate the galactic plane (GP) and supergalactic plane (SGP). White and grey hexagrams indicate the Galactic center (GC) and anti-galactic center (Anti-GC) respectively.

equal. The deficit is larger in magnitude than the excess as the expectation is N_{bg}=166.2 with an observed number of events N_{on}=147.

6.3. *Post-trial Significance*

To calculate the global post-trial significance a scan penalty must be taken for the four exposure ratios (3.35%, 6.04%, 9.58%, and 14.03%) and four energy thresholds ($10^{19.0}$, $10^{19.1}$, $10^{19.2}$, and $10^{19.3}$ eV) that were tested to maximize likelihood GOF σ_{local} of Figure 3.

Isotropic MC sets are made which have the same number of events as data for each energy threshold. The scanned variables are applied to each set to create 16 σ_{local} maps. The maximum σ_{local} significance on all 16 maps, at any grid point, is considered as one MC for counting MC sets that have a higher significance than the data.

The distribution of the maximum σ's of 2.5×10^6 MC sets that are used to calculate the post-trial significance are shown in Figure 5. There were 232 sets with a significance greater than 6.17σ. This corresponds to a global post-trial one-sided significance of $3.74\sigma_{global}$.

Though the results of previous studies, and theoretical works, could have been used as arguments for fewer scans, larger energy bins, or looser data cuts, the parameters of the analysis framework were chosen as much as possible on *a priori* considerations of statistics, detector resolution, and data/simulation agreement. The result is a conservative estimate of significance.

7. SYSTEMATIC CHECKS

There is a systematic bias on the energy determination due to seasonal and daily temperature induced changes to the average lateral distribution of particles in UHECR extensive air showers. This bias is estimated to fluctuate, about ±7%, with a negative bias in the winter months and positive in the summer. There's also an estimated fluctuation of about ±5% throughout each 24 hour period. Applying these estimated energy corrections to the data results in a lowering of the local significance by about 0.05σ.

In the calculations of the equal exposure binning, the exposure ratio, and the global significance, the trigger times of events with energies E≥$10^{17.7}$ eV were sampled to create the MC. This is to model how the TA SD would see an isotropic sky. It is known however that the acceptance, and therefore the trigger time distribution, is dependent on energy. To test the effect of this method additional MC sets were also created using uniform event trigger times and the analysis redone. The result is an increase in the pre-trial, and post-trial, significance of 0.04σ.

In addition to the seasonal energy correction test the energy distribution of events was also considered in anti-sidereal coordinates. This is an artificial coordinate system that emphasizes seasonal effects. No evidence for an energy spectrum anisotropy is found in anti-sidereal coordinates as would be expected for an anisotropy.

Other systematic checks include comparing the shower geometry variable (azimuth, zenith, core position etc.) distributions inside the anisotropic area to that outside. These show no disagreements (nor disagreements between different energy ranges inside the area). These distributions also agree with isotropic MC. The R.A., trigger time, and Dec. distributions inside the spherical cap are in good agreement between the Hotspot and Coldspot energy ranges – they also each agree with isotropic MC. Also, the full energy distributions inside, and outside, the spherical cap do not show any significant seasonal variation.

8. DISCUSSION

While there are no obvious sources directly at the energy anisotropy location, a number of supergalactic galaxy clusters such as Ursa Major (20 Mpc away), Coma (90 Mpc),

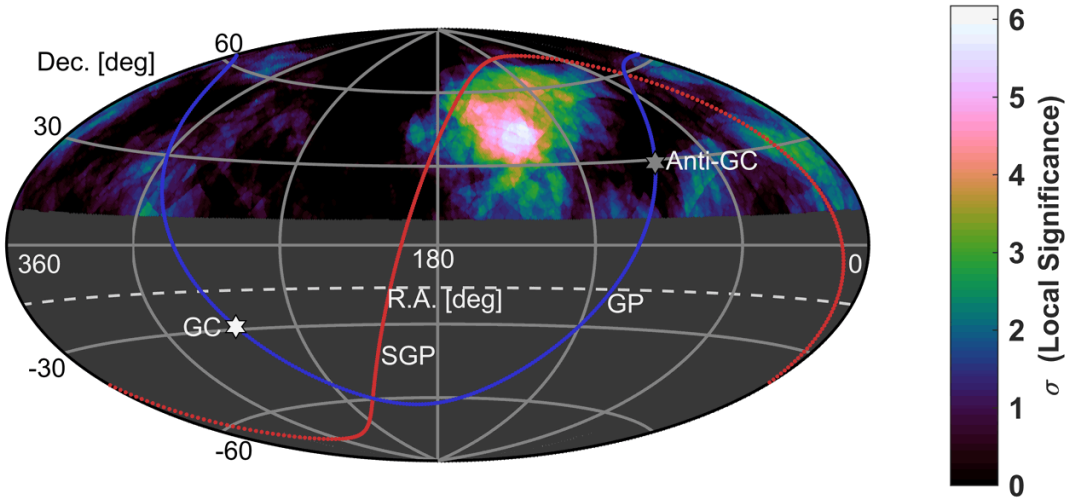

Figure 3. Projection of the energy spectrum anisotropy local pre-trial significance, for 14.03% equal exposure spherical cap bins (E≥$10^{19.2}$ eV). The maximum is 6.17σ_{local} at 9^h16^m, 45° and is 7° from the the Hotspot location of Abbasi et al. (2014a). The dashed curve at Dec. = -16° defines the FOV. Solid curves indicate the galactic plane (GP) and supergalactic plane (SGP). White and grey hexagrams indicate the Galactic center (GC) and anti-galactic center (Anti-GC).

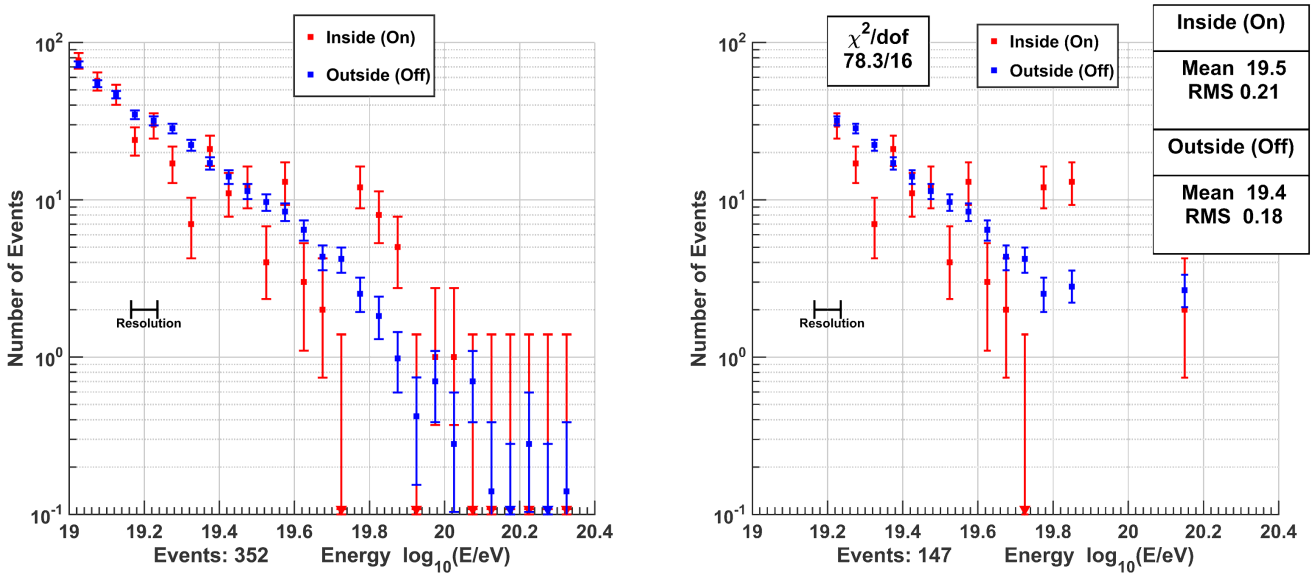

(a) (b)

Figure 4. The maximum significance energy histograms of events inside the spherical cap bin of radius 28.43° (red) compared to the expected energies (blue) at 9^h16^m, 45°. (a) Before rebinning for events with energies E>$10^{19.0}$ eV. (b) After rebinning for energies E>$10^{19.2}$ eV (the maximum significance threshold). There are 147 events with an expectation of N_{bg}=166.2. Only three out of 11 bins for E<$10^{19.75}$ eV are above expectation.

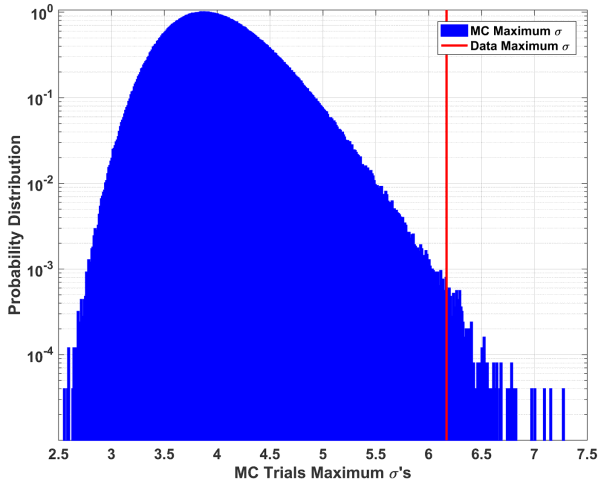

Figure 5. The distribution of the maximum local σ's for 2.5×10^6 MC trials. The area under the distribution above $6.17\sigma_{local}$ corresponds to a $3.74\sigma_{global}$ post-trial significance for the energy spectrum anisotropy.

and Virgo (20 Mpc) are nearby. If the sources are in the supergalactic plane the closest distance is 22° (in the vicinity of Ursa Major). This is about 3° further than the Hotspot location. The difference is not statistically significant given the bin sizes and Gaussian fit to the Hotspot events as shown in Abbasi et al. (2014a).

To get an idea if the measured energy spectrum anisotropy is correlated with the supergalatic plane the locations in Figure 3 with excess/deficit behavior are converted to supergalactic coordinates and fit to a straight line (weighted by the pre-trial σ^2). The result corresponds to a great-circle rotated in declination by -16.5±0.1° tilted 2±1° around the center of the fit. This is suggestive of an extended feature that could be correlated with supergalactic structure. Possible mechanisms for producing such a shift include focusing of cosmic ray flux, for events with E>50 EeV, by supergalactic magnetic sheets as discussed in Biermann et al. (1997), and deflection of lower energy events transverse to the sheet as discussed in Ryu et al. (1998).

If UHECR are protons, as indicated by previous TA studies (Abbasi et al. (2014b)), it may also be possible that this feature is associated with the closest galaxy groups and/or the Virgo cluster galaxy filaments (Dolag et al. (2004); He et al. (2016); Pfeffer et al. (2017)). In the case that the anisotropic UHECR are heavier nuclei, the deflections will be larger and their directions will be significantly impacted both by the extragalactic magnetic fields (EGMF) and the galactic magnetic halo field (GMF) (Tinyakov & Tkachev (2002); Takami et al. (2012)).

The statistical power of the current analysis is insufficient to determine the origin of this feature. It will be important to improve knowledge of mass composition of UHECR as well. Improved data on magnetic field configurations will also be important, both for galactic and extragalactic propagation. A planned expansion of the TA detector is proceeding which will increase the SD area by a factor of four (TAx4 Sagawa (2013)). Five years of data with this new detector should be sufficient to answer a number of these questions.

9. SUMMARY

Using seven years of TA SD UHECR events a feature has been found appearing as a deficit of lower energy events ($10^{19.2}$≤E<$10^{19.75}$ eV) and an excess of high energy events (E≥$10^{19.75}$ eV) in the same region of the sky. The maximum local pre-trial significance is 6.17σ and appears at 9^h16^m, 45°. The global post-trial probability of an energy spectrum anisotropy of this significance appearing by chance in an isotropic cosmic ray sky was found to be 9×10^{-5} ($3.74\sigma_{global}$). This feature is suggestive of energy dependent magnetic deflection of UHECR events.

Telescope Array is supported by the Japan Society for the Promotion of Science (JSPS) through Grants-in-Aid for Priority Area 431, Specially Promoted Research JP21000002, Scientific Research (S) JP19104006, Specially Promoted Research JP15H05693, Scientific Research (S) JP15H05741 and for Young Scientists (A) JPH26707011; by the joint research program of the Institute for Cosmic Ray Research (ICRR) and the University of Tokyo; by the U.S. National Science Foundation awards PHY-0601915, PHY-1404495, PHY-1404502, and PHY-1607727; by the National Research Foundation of Korea (2016R1A2B4014967, 2016R1A5A1013277, 2017K1A4A3015188, 2017R1A2A1A05071429); by the Russian Academy of Sciences, RFBR grant 16-02-00962a (INR), IISN project No. 4.4502.13, and Belgian Science Policy under IUAP VII/37 (ULB). The foundations of Dr. Ezekiel R. and Edna Wattis Dumke, Willard L. Eccles, and George S. and Dolores Doré Eccles all helped with generous donations. The State of Utah provided support through its Economic Development Board, and University of Utah's Office of the Vice President for Research. The experimental site became available through the cooperation of the Utah School and Institutional Trust Lands Administration (SITLA), U.S. Bureau of Land Management (BLM), and the U.S. Air Force. We appreciate the assistance of the State of Utah and Fillmore offices of the BLM in crafting the Plan of Development for the site. Patrick Shea assisted the collaboration with valuable advice. The people and officials of Millard County, Utah have provided greatly appreciated steadfast support. We are indebted to the Millard County Road Department for maintenance of the sites roads. We are grateful for the contributions of our home institutions technical staffs and the

University of Utah Center for High Performance Computing for the allocation of computer time.

REFERENCES

Abbasi, R. U., et al. 2008, PhRvL, 100, 101101. https://arxiv.org/abs/astro-ph/0703099

—. 2014a, ApJ, 790, L21. https://arxiv.org/abs/1404.5890

—. 2014b, Astropart. Phys., 64, 49. https://arxiv.org/abs/1408.1726

—. 2015, Astropart. Phys., 68, 27 . https://arxiv.org/abs/1410.3151

Abu-Zayyad, T., et al. 2013a, Nucl. Instrum. Meth., A689, 87. https://arxiv.org/abs/1201.4964

—. 2013b, ApJ, 768, L1. https://arxiv.org/abs/1205.5067

—. 2013c, ApJ, 777, 88. https://arxiv.org/abs/1306.5808

Ajello, M., Alexander, D. M., Greiner, J., et al. 2012, ApJ, 749, 21. https://arxiv.org/abs/1202.3137

Baker, S., & Cousins, R. D. 1984, Nucl. Instr. Meth. Phys. Res., 221, 437

Biermann, P. L., Kang, H., & Ryu, D. 1997, 9 p. https://arxiv.org/abs/astro-ph/9709250

Dolag, K., Grasso, D., Springel, V., & Tkachev, I. 2004, J. Korean Astron. Soc., 37, 427

Gillessen, S., & Harney, H. L. 2005, A&A, 430, 355. https://arxiv.org/abs/astro-ph/0411660

Hayashida, N., et al. 1999a, Astropart. Phys., 10, 303. https://arxiv.org/abs/astro-ph/9807045

Hayashida, N., et al. 1999b, in Proceedings, 26th ICRC, Salt Lake City, August 17-25. http://krusty.physics.utah.edu/~icrc1999/root/vol3/o1_3_04.pdf

He, H.-N., Kusenko, A., Nagataki, S., et al. 2016, PhRvD, D93, 043011. https://arxiv.org/abs/1411.5273

Heinrich, J. G. 2001, CDF, Note 5718

Ivanov, D. 2012, PhD thesis, Rutgers, the State University of New Jersey. http://www.telescopearray.com/images/papers/theses/thesis_ivanov_rev2016.pdf

Ivanov, D., & Thomson, G. B. 2008, ICRC, 4, 445

Kawata, K., Fukushima, M., & D., I. 2013, in Proceedings, 33rd ICRC (ICRC2013): Rio de Janeiro, Brazil, July 2-9, 0311. http://www.cbpf.br/~icrc2013/papers/icrc2013-0311.pdf

Kotera, K., & Olinto, A. V. 2011, ARA&A, 49, 119. https://arxiv.org/abs/1101.4256

Li, T. P., & Ma, Y. Q. 1983, ApJ, 272, 317

Lundquist, J. P. 2017, in Proceedings, 35th ICRC (ICRC2017): Busan, South Korea, August 12-20, 513. https://pos.sissa.it/301/513/pdf

Olive, K. A., et al. 2014, Chin. Phys., C38, 090001

Pfeffer, D. N., Kovetz, E. D., & Kamionkowski, M. 2017, Mon. Not. Roy. Astron. Soc., 466, 2922. https://arxiv.org/abs/1512.04959

Ryu, D., Kang, H., & Biermann, P. L. 1998, A&A, 335, 19. https://arxiv.org/abs/astro-ph/9803275

Sagawa, H. 2013, in Proceedings, 33rd ICRC (ICRC2013): Rio de Janeiro, Brazil, July 2-9, 0121. http://www.cbpf.br/~icrc2013/papers/icrc2013-0121.pdf

Takami, H., Inoue, S., & Yamamoto, T. 2012, Astropart. Phys., 35, 767. https://arxiv.org/abs/1202.2874

Tinyakov, P. G., & Tkachev, I. I. 2002, Astropart. Phys., 18, 165. https://arxiv.org/abs/astro-ph/0111305

Tokuno, H., et al. 2012, Nucl. Instrum. Meth., A676, 54. https://arxiv.org/abs/1201.0002

Vallado, D. A. 2007, Fundamentals of Astrodynamics and Applications (Springer-Verlag New York), 1055. https://books.google.com/books?id=PJLlWzMBKjkC